Supplementary material

Image acquisition

A representative MRI protocol from one centre included the following image acquisitions:

(1) 2D T1-weighted: TR= 30 milliseconds, TE= 11.0 milliseconds, slice thickness= 3.0mm, imaging frequency= 63.43, acquisition matrix= 0x256x192x0, flip angle= 30.0, number of phase encoding steps= 192, FoV= 187*250mm;

(2) 2D fast fluid- attenuated inversion recovery (2D FLAIR): with voxel size= 0.98 × 0.98, TR= 2980.0 milliseconds, TE = 12 milliseconds, slice thickness= 3.0mm, imaging frequency= 63.643, number of phase encoding steps= 258, matrix size = 0x256x256x0, flip angle= 180.0, FoV= 250*250mm;

(3) 2D T2-weighted: with voxel size= 0.98 × 0.98, TR= 5750.0 milliseconds, TE = 86 milliseconds, slice thickness = 3.0mm, imaging frequency= 63.643, number of phase encoding steps= 259, matrix size = 0x256x256x0, flip angle= 180.0, FoV= 250*250mm;

(4) 2D proton density (PD): with voxel size= 0.98 × 0.98, TR= 2980.0 milliseconds, TE = 12 milliseconds, slice thickness = 3.0mm, imaging frequency= 63.643, number of phase encoding steps= 258, matrix size = 0x256x256x0, flip angle= 180.0, FoV= 250*250mm;

Participants underwent either 1.5 or 3.0 Tesla.

MANUFACTURER	**MAGNETIC FIELD**			
	1.5 T	3.0 T	Missing	**TOTAL**
GE MEDICAL SYSTEMS	293	46	-	339
Marconi Medical Systems, Inc.	5	-	-	5
Philips Medical Systems	153	70	-	223
SIEMENS	366	51	-	417
TOSHIBA_MEC	-	-	3	3
Missing	-	1	-	1
TOTAL	817	168	3	988

Study-specific template construction

We randomly selected 39 subjects to create a study-specific template in ANTs. The number of subject was chosen to be as large as feasible, based on computation time, and as significantly larger than previous cohorts used for this purpose (e.g., N= 19 (Eshaghi et al., 2014), N= 20 (Whitwell *et al.*, 2007)).

Gender (M/F)	29/ 10
Age (mean±SD)	46.78±6.45
Trial Arm (DMT/Placebo)	420/422
EDSS (median, range)	6 (3-7)
SDMT (mean±SD)	40.04±15.70
9HPT (mean±SD)	32.17±13.29

We interpolated the T1w lesion filled scans to 1x1x1mm, and registered them using a rigid body transformation to the MNI152 space (http://www.bic.mni.mcgill.ca/ServicesAtlases/ICBM152NLin2009).

MANUFACTURER	MAGNETIC FIELD		
	1.5 T	3.0 T	TOTAL
GE MEDICAL SYSTEMS	8	1	9
Marconi Medical Systems, Inc.	2	0	2
Philips Medical Systems	9	5	14
SIEMENS	11	3	14
TOSHIBA_MEC	-	-	-
Missing	-	-	-
TOTAL	30	9	39

To determine whether the randomly selected sub-sample was representative of the cohort, we performed two-sample Kolmogorov-Smirnov test for continuous variables, and two-sample test for equality of proportions for the categorical ones. The randomly selected sub-sample did not significantly differ from the entire cohort when considering age (D= 0.11, p= 0.72), baseline mean whole brain GM volume (D= 0.10, p= 0.85), baseline mean DGM volume measures (D= 0.13, p= 0.56), mean 9HPT score (D= 0.17, p= 0.28), mean SDMT score (D=

0.18, p= 0.75), and EDSS (D= 0.11, p= 0.80). The proportion of participants scanned at 1.5 and 3T did not differ in the two samples (respectively, X^2 = 0.86, df = 1, p= 0.35, CI [-0.19:0.077], and X^2 =0.97, df = 1, p= 0.33, CI [-0.07: 0.20]). The proportion of females and males in the two samples did not differ (respectively, X^2 = 2.10, df = 1, p= 0.15, CI [-0.03: 0.25], and X^2 = 2.10, df = 1, p= 0.15, CI [-0.25: 0.03]).

Whole brain mask

We created a whole brain mask to: (1) to constrain the ICA to the parenchymal brain, and (2) identify and label brain regions involved in each ICA-component. We used the majority voting algorithm implemented in antsJointLabelFusion to fuse the 39 parcellation maps of subjects that had contributed to the template and obtain a single parcellation map where the likelihood that each region corresponds to the labelled one is higher (H. Wang et al., 2013; H. Wang & Yushkevich, 2013). We used this atlas-mask to label brain regions involved in each component. We excluded brain structures from the brain mask (e.g., ventricles, meninges, etc.), binarised the output and used the obtained mask to mask the processed GM probability maps and reduce the computational expense of the ICA.

Association across baseline regional volumes and ICA loadings

We determined the association of each ICA-components with baseline volume of the encompassed brain regions as follows. From the pre-processing stage, for each participant we obtained a parcellation map, and estimated the baseline volume measure of whole brain GM and of single brain regions (higher values correspond to bigger volumes). By overlaying the identified ICA-components with the whole brain mask created from the parcellation maps (as described above), we determined which brain regions were involved in each component. We correlated the loading of ICA-components (generated from baseline scans) with the volume of each brain region encompassed by the GM pattern. In this way, we could determine which brain regions in each component presented a positive correlation with the baseline volume of that region (higher baseline volume higher loading) and which presented a negative correlation (higher baseline volume, lower loading).

ICA in healthy controls

To determine whether similar components to the ones identified in patients with SPMS were present in HCs, we randomly selected a sample of 400 participants from the Human Connectome Project. We applied the same pipeline to analyse T1 and T2 scans. To increase the accuracy of the registrations, we substituted the customised study specific template (created from participants with MS and reconstructed 2D scans), with the MNI template (created from 3D images of healthy controls). To determine whether the same components were present in healthy controls and in patients with MS, we visually inspected the resulting ICA components and calculated spatial cross-correlations.

Components	Correlation
1	0.31
2	0.65
3	0.52
5	0.35
6	0.30
7	0.31
8	0.55
9	0.41
11	0.55
12	0.23
13	0.66
15	0.28
17	0.38
18	0.17
20	0.61

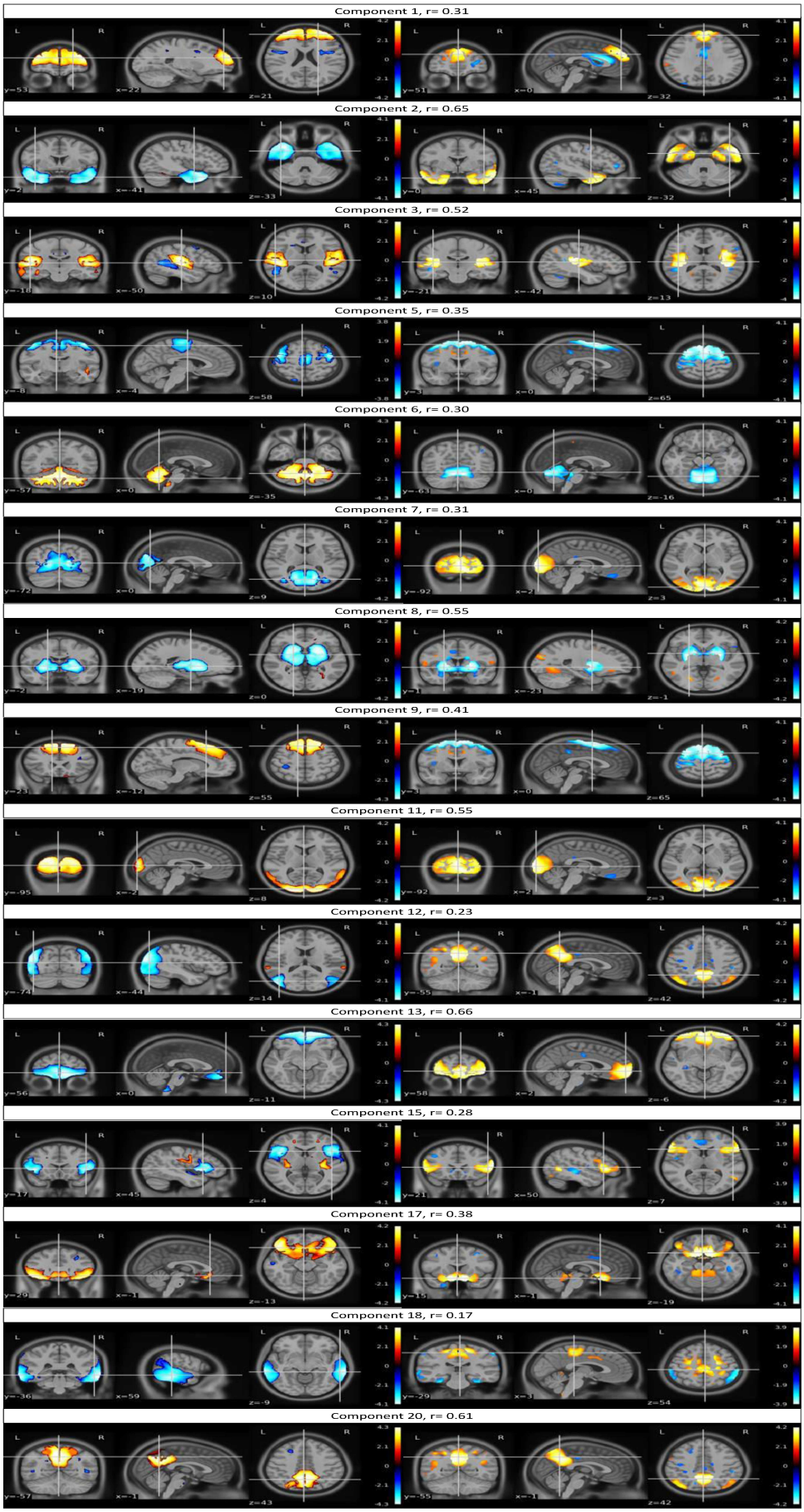
Component 1, r= 0.31
Component 2, r= 0.65
Component 3, r= 0.52
Component 5, r= 0.35
Component 6, r= 0.30
Component 7, r= 0.31
Component 8, r= 0.55
Component 9, r= 0.41
Component 11, r= 0.55
Component 12, r= 0.23
Component 13, r= 0.66
Component 15, r= 0.28
Component 17, r= 0.38
Component 18, r= 0.17
Component 20, r= 0.61

Nine GM patterns identified from patients with SPMS were uniquely correlated and present also in HCs, suggesting that they are not disease specific. Although slightly overlapping with HC patterns, two SPMS ICA-components (component 12 and 18) were detected in patients with MS but not in HCs, which might be disease specific.

Supplementary Tables

Table s1. *Results of the spatial cross-correlations between the 20 components obtained in each of the four sub-sample and from the entire cohort*

Network	Sub-sample 1 vs. 2	Sub-sample 1 vs. 3	Sub-sample 1 vs.4	Entire cohort vs. sub-sample 1	Sub-sample 2 vs. 3	Sub-sample 2 vs. 4	Entire cohort vs. sub-sample 2	Sub-sample 3 vs. 4	Entire cohort vs. sub-sample 3	Entire cohort vs. sub-sample 4
1	0.86	0.80	0.84	0.89	0.82	0.88	0.91	0.82	0.84	0.88
2	0.88	0.88	0.87	0.90	0.92	0.90	0.95	0.89	0.93	0.92
3	0.41	0.30	0.52	0.35	0.66	0.36	0.54	0.48	0.63	0.73
5	0.37	0.61	0.50	0.43	0.28	0.16	0.41	0.40	0.42	0.14
6	0.94	0.94	0.93	0.94	0.95	0.95	0.97	0.94	0.95	0.96
7	0.10	0.27	0.20	0.22	0.55	0.51	0.63	0.60	0.73	0.75
8	0.93	0.90	0.88	0.95	0.88	0.93	0.95	0.82	0.90	0.91
9	0.62	0.61	0.64	0.75	0.56	0.69	0.77	0.62	0.72	0.76
11	0.78	0.62	0.41	0.78	0.53	0.35	0.74	0.53	0.81	0.52
12	0.48	0.69	0.47	0.82	0.51	0.20	0.55	0.24	0.83	0.39
13	0.85	0.78	0.86	0.92	0.76	0.83	0.89	0.77	0.82	0.90
15	0.41	0.42	0.52	0.52	0.20	0.33	0.18	0.43	0.69	0.59
17	0.40	0.63	0.60	0.69	0.52	0.46	0.51	0.66	0.81	0.71
18	0.63	0.51	0.44	0.53	0.55	0.61	0.61	0.33	0.82	0.36
20	0.69	0.67	0.62	0.72	0.80	0.70	0.81	0.75	0.90	0.80

Table legend: The table reports the spatial cross-correlations results for the stable ICA-components (i.e., showed a statistically significant correlations ($p<0.05$) in all 4 folds and in the entire cohort).

Table s2. *Results of the spatial cross-correlations across the 15 stable components obtained from the entire cohort and those obtained in each of the five cross-validation folds (based on acquisition region).*

COMPONENTS	NORTHERN AMERICA	NORTHERN EUROPE	SOUTHERN EUROPE	EASTERN EUROPE	WESTERN EUROPE
V1	0.68	0.91	0.68	0.68	0.81
V2	0.89	0.93	0.80	0.88	0.89
V3	0.68	0.72	0.19	0.66	0.53
V5	0.22	0.24	0.20	0.51	0.21
V6	0.95	0.90	0.76	0.96	0.93
V7	0.71	0.68	0.54	0.84	0.41
V8	0.93	0.84	0.86	0.94	0.84
V9	0.35	0.73	0.39	0.29	0.11
V11	0.83	0.76	0.79	0.83	0.82
V12	0.58	0.63	0.40	0.79	0.70
V13	0.54	0.74	0.69	0.82	0.70
V15	0.46	0.17	0.24	0.21	0.24
V17	0.42	0.42	0.27	0.85	0.64
V18	0.11	0.62	0.21	0.77	0.44
V20	0.35	0.80	0.52	0.84	0.71

Table s3. *Results of the spatial cross-correlations across the 15 stable components obtained from the entire cohort and those obtained in each of the three cross-validation folds (acquisition manufacturer).*

COMPONENTS	SIEMENS	GE	PHILIPS
V1	0.85	0.85	0.78
V2	0.96	0.92	0.91
V3	0.61	0.71	0.63
V5	0.36	0.43	0.35
V6	0.98	0.97	0.88
V7	0.86	0.75	0.69
V8	0.92	0.94	0.64
V9	0.36	0.82	0.19
V11	0.66	0.74	0.75
V12	0.46	0.53	0.60
V13	0.96	0.90	0.83
V15	0.52	0.68	0.40
V17	0.83	0.76	0.37
V18	0.59	0.66	0.62
V20	0.83	0.90	0.69

Table legend: The spatial cross-correlations results for the stable ICA-components (i.e., showed a statistically significant correlations ($p<0.05$) between the entire cohort and the 5 cross-validation folds representing the acquisition manufacturer).

Table s4. *List of the 15 stable components with their corresponding involved brain regions*

Networks	Regions
Component 1	▲Superior frontal gyrus, ▲Middle frontal gyrus, ▲Superior frontal gyrus medial segment, ▲Anterior cingulate gyrus, ▲Opercular part of the inferior frontal gyrus
Component 2	▼Temporal pole, ▼Inferior temporal gyrus, ▼Middle temporal gyrus, ▼Middle cingulate gyrus, ▼Parahippocampal gyrus, ▼Precentral gyrus medial segment, ▼Posterior cingulate gyrus, ▼Entorhinal area, ▼Parietal lobule, ▼ Fusiform gyrus
Component 3	▲Parietal and ▲Temporal pole, ▲Middle temporal gyrus, ▲Superior temporal gyrus, ▲Planum temporale, ▲ Parietal operculum, ▲Planum polare, ▲Central operculum, ▲Middle cingulate gyrus, ▲Cingulate, ▲Middle frontal gyrus, ▲Posterior Insula, ▲Transverse temporal gyrus
Component 5	▼Middle temporal gyrus, ▼Parietal lobule, ▼Supramarginal gyrus, ▼Postcentral gyrus, ▼Precentral gyrus, ▼ Triangular part of the inferior frontal gyrus, ▼Middle frontal gyrus, ▲Superior temporal gyrus, ▼Angular gyrus, ▼ Cuneus, ▼Superior frontal gyrus, ▼Precentral gyrus medial segment, ▼Inferior occipital gyrus
Component 6	▲Cerebellum, ▲Brain Stem, ▲Pons, ▼Lingual gyrus, ▼Fusiform gyrus, ▼Temporal and ▼Parietal lobe
Component 7	▼Superior occipital gyrus, ▼Occipital lobe, ▼Lingual gyrus, ▼Calcalcarine cortex, ▼Precuneus, ▼Parietal lobe, ▼Temporal lobe, ▲Middle temporal gyrus, ▼Frontal lobe, ▲Precentral gyrus, ▼Supramarginal gyrus
Component 8	▼Brain Stem, ▼Pons, ▼Ventral DC, ▼Thalamus, ▼Insula, ▼Accumbens, ▼Caudate, ▼Putamen, ▼Pallidum, ▼ Frontal and ▲Temporal lobe
Component 9	▲Angular gyrus, ▲Middle occipital gyrus, ▲Postcentral gyrus, ▲Medial orbital gyrus, ▲Triangular part of the inferior frontal gyrus, ▲Middle frontal gyrus, ▲Superior frontal gyrus medial segment, ▲Superior frontal gyrus, ▲ Superior parietal lobule, ▲Claustrum, ▲Occipital, ▲Frontal, and ▲Parietal pole
Component 11	▲Occipital pole, ▲Calcarine cortex, ▲Cuneus, ▼Middle temporal gyrus, ▼Inferior temporal gyrus, ▲Inferior occipital gyrus, ▼Angular gyrus, ▼Superior parietal lobule, ▼Supramarginal gyrus
Component 12	▼Angular gyrus, ▼Inferior temporal gyrus, ▼Middle temporal gyrus, ▼Inferior occipital gyrus, ▼Middle occipital gyrus, ▼Superior occipital gyrus, ▼Fusiform gyrus, ▼Occipital fusiform gyrus, ▼Precentral gyrus, ▼Middle frontal gyrus, ▼Claustrum, ▼Superior frontal gyrus
Component 13	▼Lateral orbital gyrus, ▼Middle frontal gyrus, ▼Superior frontal gyrus, ▼Superior frontal gyrus medial segment, ▼ Anterior orbital gyrus, ▼Medial frontal cortex, ▼Gyrus rectus, ▼Frontal pole, ▼Medial orbital gyrus, ▼Anterior cingulate gyrus, ▼Brain Stem, ▼Lingual gyrus, ▼Temporal pole
Component 15	▲Thalamus, ▲Caudate, ▼Anterior insula, ▼Posterior insula, ▼Planum polare, ▲Putamen, ▼Frontal operculum, ▼Planum temporale, ▼Claustrum, ▼Triangular part of the inferior frontal gyrus, ▼Opercular part of the inferior frontal gyrus, ▲Precentral gyrus, ▼Central operculum, ▼Parietal operculum, ▼Frontal and ▼Temporal pole
Component 17	▲Hippocampus, ▲Pons, ▲Middle temporal gyrus, ▲Superior temporal gyrus, ▲Postcentral gyrus, ▲Triangular part of the inferior frontal gyrus, ▲Temporal pole, ▲Posterior orbital gyrus, ▲Medial orbital gyrus, ▲Anterior insula, Claustrum, ▲Basal Forebrain, ▲Putamen, ▲Subcallosal area, ▲Medial orbital gyrus, ▲Gyrus rectus, ▲Medial frontal cortex, ▲Lateral orbital gyrus, ▲Orbital part of the inferior frontal gyrus, ▲Medial frontal cortex, ▲Anterior

	cingulate gyrus, ▲Anterior orbital gyrus, ▲Posterior cingulate gyrus, ▲Postcentral gyrus, ▲Frontal operculum, ▲ Inferior temporal gyrus
Component 18	▼Middle occipital gyrus, ▼Postcentral gyrus, ▼Precentral gyrus, ▼Opercular part of the inferior frontal gyrus, ▼ Fusiform gyrus, ▼Parahippocampal gyrus, ▼Frontal, ▼Occipital and ▼Parietal lobe, ▼Inferior temporal gyrus, ▼ Middle temporal gyrus, ▼Superior temporal gyrus, ▼Supramarginal gyrus, ▼Middle temporal gyrus
Component 20	▲Superior occipital gyrus, ▲Superior parietal lobule, ▲Precuneus, ▲Posterior cingulate gyrus, ▲Superior frontal gyrus, ▲Middle frontal gyrus, ▲Angular gyrus, ▲Occipital lobule

▲ Relative preserved brain region

▼ Atrophic brain region

Table legend: We overlaid a whole brain parcellation mask with the identified ICA-components in order to retrieve and label brain regions involved in each network. We correlated the loading of ICA-components with the baseline volume of the areas involved in each network to identify which brain area in each network showed volume loss (negative correlation between network loading and baseline volume) and which represented relative brain preservation (negative correlation between those volumes and ICA-loadings).

Table s5. *Correlations between the loading values of ICA-components and whole brain GM volumes, SDMT, EDSS, and 9HPT score*

GM NETWORKS	WHOLE BRAIN GM VOLUME	EDSS N= 830	9HPT N= 829	SDMT N= 391
Component 1	r= 0.08 95% CI [0.01:0.14] p= 0.28	rho= - 0.01 p= 0.79	r= 0.13 95% CI [0.06: 0.19] p< 0.01*	r= 0.22 95% CI [0.13:0.32] p<0.001*
Component 2	r= - 0.25 95%CI [-0.3:-0.19] p<0.001*	rho= 0.08 p= 0.15	r= -0.04 95% CI [-0.11: 0.03] p= 0.33	r= - 0.07 95% CI [- 0.17:0.03] p= 1
Component 3	r= 0.18 95%CI [0.11:0.23] p<0.001*	rho= - 0.05 p= 0.22	r= 0.05 95% CI [-0.02:0.11] p= 0.31	r= 0.04 95% CI [- 0.06:0.14] p= 1
Component 5	r= - 0.16 95%CI [-0.22:-0.09] p<0.001*	rho= - 0.03 p= 0.39	r= 0.05 95% CI [- 0.02: 0.11] p= 0.35	r= 0.07 95% CI [- 0.03:0.16] p= 1
Component 6	r= - 0.09 95% CI [-0.15:-0.02] p=0.10	rho= - 0.11 p= 0.02*	r= 0.19 95% CI [0.12: 0.25] p <0.001*	r= 0.10 95% CI [0:0.19] p= 1
Component 7	r= - 0.07 95% CI [-0.13:-0.01] p= 0.38	rho= 0.04 p= 0.36	r= 0.02 95% CI [- 0.05: 0.09] p= 0.63	r= - 0.06 95% CI [- 0.16:0.04] p= 1
Component 8	r= - 0.18 95% CI [-0.24:-0.12] p<0.001*	rho= 0.06 p= 0.22	r= -0.32 95% CI [-0.38:-0.25] p<0.001*	r= - 0.44 95% CI [- 0.52: - 0.36] p<0.001*
Component 9	r= 0.20 95% CI	rho= 0.06	r= -0.06 95% CI	r= - 0.01 95% CI

	[0.14:0.26] p<0.001*	p= 0.21	[-0.13:0.01] p= 0.21	[- 0.11:0.09] p= 1
Component 11	r= - 0.12 95% CI [-0.17:-0.05] p<0.01*	rho= 0.07 p= 0.12	r= 0.11 95% CI [0.04: 0.17] p< 0.01*	r= 0.16 95% CI [0.06:0.25] p<0.05*
Component 12	r= - 0.17 95% CI [-0.23:-0.11] p<0.001*	rho= - 0.04 p= 0.35	r= -0.03 95% CI [- 0.09:0.04] p= 0.56	r= - 0.12 95% CI [- 0.21: -0.02] p=0.39
Component 13	r= - 0.38 95% CI [-0.43:-0.33] p<0.001*	rho= 0.07 p= 0.16	r= -0.06 95% CI [- 0.12:0.01] p= 0.24	r= - 0.12 95% CI [- 0.21: - 0.02] p=0.39
Component **1**5	r= - 0.01 95% CI [-0.07:0.06] p= 1	rho= 0.07 p= 0.18	r= -0.04 95% CI [- 0.11:0.03] p= 0.36	r= - 0.13 95% CI [- 0.23: - 0.03] p= 0.21
Component **1**7	r= 0.19 95% CI [0.13:0.25] p<0.001*	rho= 0.02 p= 0.65	r= 0.02 95% CI [- 0.05:0.09] p= 0.61	r= 0.03 95% CI [- 0.07:0.13] p= 1
Component **1**8	r= - 0.28 95% CI [-0.33:-0.22] p<0.001*	rho= 0.08 p= 0.19	r= - 0.03 95% CI [- 0.09: 0.04] p= 0.53	r= - 0.15 95% CI [- 0.25: - 0.05] p<0.05*
Component 20	r= 0.28 95% CI [0.22:0.33] p<0.001*	rho= 0.05 p= 0.22	r= 0.08 95% CI [0.01: 0.15] p= 0.08	r= 0.18 95% CI [0.08: 0.27] p<0.01*

Acronyms: GM= grey matter, EDSS= expanded disability status scale; 9HPT= nine hole peg test; SDMT= symbol digit modalities test; CI= confidence interval

*Statistically significant after Bonferroni correction

We report the Bonferroni Adjusted P values

Table s6. *Correlations across the SDMT, EDSS, and 9HPT score at baseline and the lesion load, DGM, GM, and thalamus volumes.*

MRI MEASURES	EDSS N= 830	9HPT N= 829	SDMT N= 391
Whole brain GM	rho= - 0.09 p= 0.052	r= 0.08 95% CI [0.01: 0.14] p<0.05*	r= 0.22 95% CI [0.12:0.31] p= 0.18
Deep GM	rho= - 0.07 p<0.05*	r= 0.06 95% CI [- 0.01:0.13] p= 0.09	r= 0.13 95% CI [0.03:0.23] p<0.001**
Lesion load	rho= 0.07 p= 0.06	r= -0.29 95% CI [-0.35:-0.23] p< 0.001*	r= -0.43 95% CI [-0.51:-0.35] p<0.001*
Thalamus	rho= - 0.12 p< 0.005*	r= 0.27 95% CI [0.21: 0.33] p<0.001*	r= 0.41 95% CI [0.32:0.49] p<0.001*

Acronyms: GM= grey matter, EDSS= expanded disability status scale; 9HPT= nine-hole peg test; SDMT= symbol digit modalities test; CI= confidence interval

*Statistically significant after Bonferroni correction

We report the Bonferroni Adjusted P values

Table s7. *Survival analysis for the EDSS, 9HPT, and SDMT progression*

Predictors	EDSS progression confirmed at 3 months			20% 9HPT worsening			10% SDMT worsening		
Brain regions	**HR**	**95% CI**	**p-value**	**HR**	**95% CI**	**p-value**	**HR**	**95% CI**	**p-value**
Component 1	1.00	0.86-1.16	0.97	1.18	0.96-1.45	0.11	0.85	0.72-1.01	0.06
Component 2	1.10	0.94-1.27	0.24	1.30	1.06-1.60	0.01**	1.03	0.86-1.22	0.76
Component 3	1.02	0.88-1.17	0.82	1.03	0.86-1.25	0.73	0.97	0.82-1.15	0.69
Component 5	0.90	0.78-1.04	0.15	0.92	0.76-1.11	0.38	1.07	0.91-1.26	0.44
Component 6	1.04	0.90-1.20	0.64	0.88	0.72-1.08	0.21	0.97	0.81-1.16	0.74
Component 7	1.05	0.91-1.21	0.50	0.86	0.72-1.03	0.10	0.82	0.71-0.96	0.01*
Component 8	1.04	0.90-1.20	0.58	1.02	0.84-1.24	0.84	1.29	1.09-1.52	p<0.003***
Component 9	0.98	0.84-1.13	0.75	0.95	0.77-1.16	0.58	0.91	0.76-1.09	0.30
Component 11	0.98	0.85-1.14	0.82	1.03	0.85-1.24	0.76	0.93	0.78-1.12	0.46
Component 12	1.01	0.88-1.17	0.88	0.85	0.71-1.02	0.08	1.14	0.96-1.34	0.13
Component 13	1.01	0.87-1.16	0.95	0.94	0.78-1.13	0.49	1.28	1.08-1.51	p<0.005***
Component 15	0.99	0.86-1.14	0.87	1.07	0.89-1.28	0.50	1.25	1.05-1.50	0.01**
Component 17	0.97	0.84-1.12	0.68	0.89	0.74-1.07	0.22	0.84	0.71-0.99	0.04*
Component 18	1.08	0.94-1.25	0.30	1.14	0.95-1.36	0.17	1.18	1.00-1.40	0.046*
Component 20	1.05	0.91-1.21	0.55	1.21	1.01-1.45	0.04*	1.00	0.85-1.17	0.96
Whole GM	0.98	0.61-1.02	0.07	0.90	0.71-1.14	0.38	0.83	0.67-1.03	0.09
DGM	0.79	0.81-1.19	0.86	0.72	0.52-0.99	0.05*	0.95	0.71-1.26	0.72
Lesion load	0.99	0.87-1.12	0.83	0.98	0.82-1.16	0.79	1.32	1.16-1.50	p<0.001****
Thalamus	0.96	0.81-1.14	0.63	1.01	0.81-1.26	0.90	0.82	0.68-1.00	0.048*

*Caption: *p<0.05 ** p<0.01 ***p<0.005 ****p<0.001*

Table legend: We report here the results for the univariate Cox regression models for all the assessed independent variables (predictors). For each standard deviation unit decrease in the baseline caudate volume the risk of developing a confirmed disability progression increased by the 19%. Two ICA-components (component 2 and component 20), and the baseline volume of the DGM predicted the 20% worsening of the 9HPT. Six ICA-components, lesion load, and the volume of the thalamus predicted the 10% SDMT worsening.

Acronyms: EDSS= expanded disability status scale; 9HPT= nine-hole peg test; SDMT= symbol digit modalities test; HR= hazard ratio, CI= confidence interval; DGM= deep grey matter

Figure s1. *Cumulative hazard function for the EDSS progression confirmed at 3 months.*

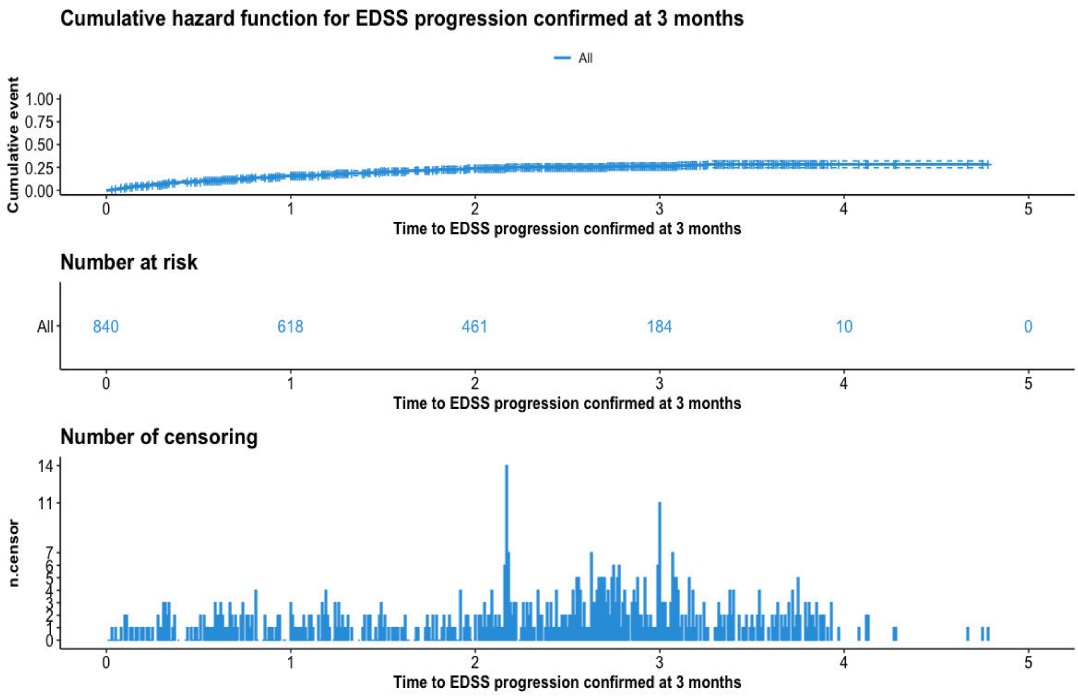

Figure legend: The figure shows the cumulative hazard function for the EDSS progression confirmed at 3 months. By the end of the study, the 28.5% of patients reported a 12-week confirmed EDSS progression. The number of censored and the number of subjects at risk of developing the EDSS progression at each timepoint are also reported

Figure s2. *Cumulative hazard function for the 20% 9HPT worsening*

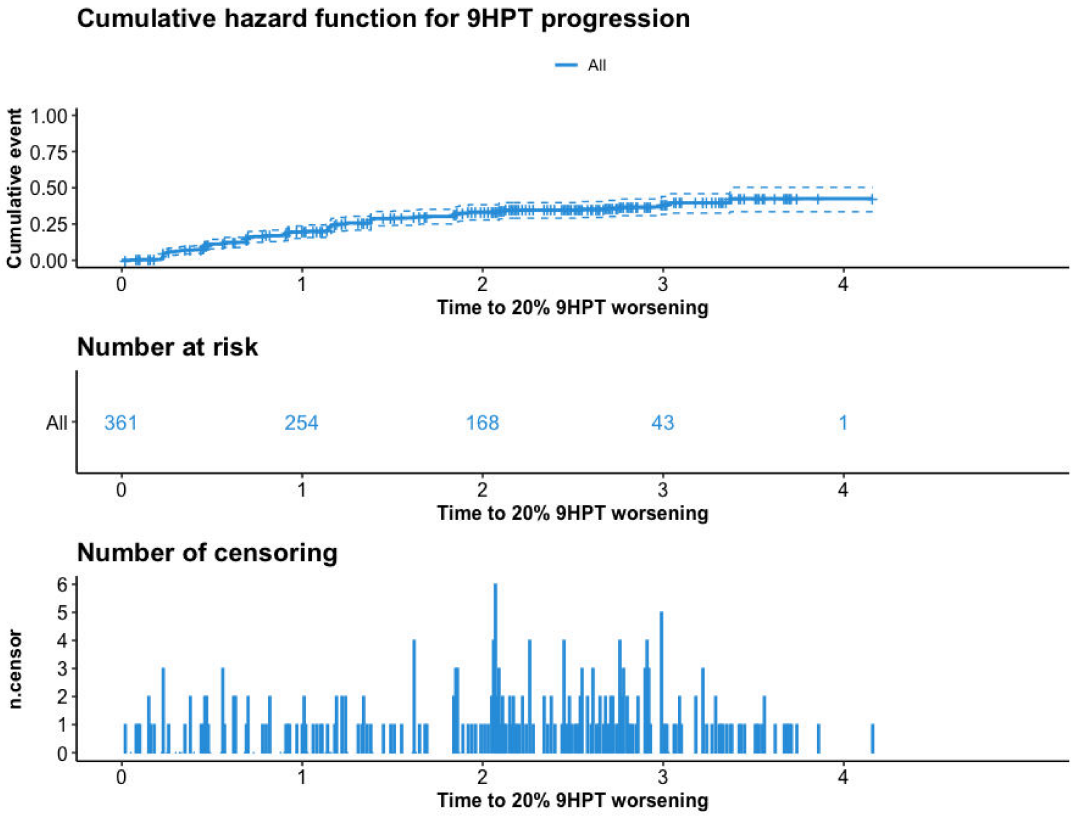

Figure legend: The figure shows the cumulative hazard function for the 20% 9HPT worsening. By the end of the study, the 42% of patients reported a 9HPT progression. The number of censored and the number of subjects at risk of developing the 9HPT progression at each timepoint are also reported

Figure s3. *Cumulative hazard function for the 10% SDMT worsening*

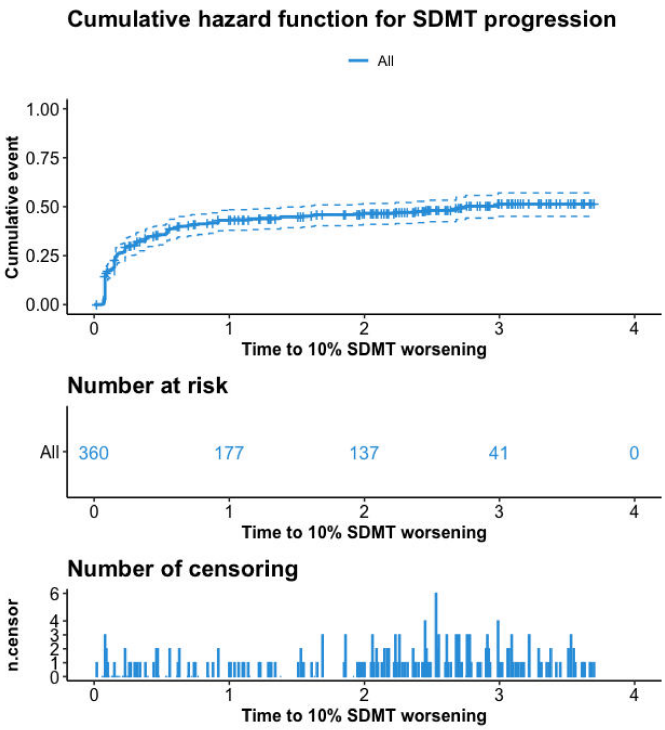

Figure legend: The figure shows the cumulative hazard function for the 10% SDMT worsening. By the end of the study, the 51% of subjects reported a SDMT progression. The number of censored and the number of subjects at risk of developing the SDMT progression at each timepoint are also reported